Carbohydrate Polymers 83 (2011) 1775–1786

Contents lists available at ScienceDirect

Carbohydrate Polymers

journal homepage: www.elsevier.com/locate/carbpol

Starch granule characterization by kinetic analysis of their stages during enzymic hydrolysis: ^{1}H nuclear magnetic resonance studies

Anthony C. Dona[a,b], Guilhem Pages[a], Robert G. Gilbert[b], Philip W. Kuchel[a,*]

[a] School of Molecular Bioscience, University of Sydney, NSW 2006, Australia
[b] Centre for Nutrition and Food Sciences, Hartley Teakle Building 83, The University of Queensland, Brisbane, QLD 4072, Australia

ARTICLE INFO

Article history:
Received 31 August 2010
Received in revised form 15 October 2010
Accepted 19 October 2010
Available online 28 October 2010

Keywords:
α-Amylase (E.C. 3.2.1.1)
Glucoamylase (E.C. 3.2.1.3)
Digestion kinetics
Product inhibition
Rapidly digested starch
Slowly digested starch
Michaelis–Menten kinetics
Time-resolved nuclear magnetic resonance spectroscopy
NMR

ABSTRACT

^{1}H nuclear magnetic resonance (NMR) spectroscopy was used to study the kinetics of digestion of starch by two hydrolytic enzymes; specifically we studied the reactions of α-amylase from *B. licheniformis* (E.C. 3.2.1.1) and glucoamylase from *Aspergillus niger* (E.C. 3.2.1.3) with starch granules (early stages of digestion) and with oligosaccharides (a later stage). This was done to provide a characterization of starch granules from various sources, with respect to the kinetics of glucose release from them. For the smaller oligosaccharides, α-amylase was inhibited by its reaction product maltose, while glucoamylase was not inhibited by its main product, glucose. The hydrolysis of oligosaccharides up to seven glucose units in length (maltoheptaose) followed Michaelis–Menten kinetics. For starch granules, experimental evidence suggests that the digestion kinetics changes subsequent to the hydrolysis of starch chains, which are accessible to enzymic attack. The rapid-digestion stage, consisting of enzymic attack on accessible starch chains, was precisely described by classical Michaelis–Menten kinetics, without considering product inhibition. During the slow-digestion stage, the rate decreased significantly; this is posited as being due to the inaccessibility of inter-glucose linkages becoming the rate-determining step.

1. Introduction

The rate of starch digestion, and hence glucose absorption into the cardiovascular system, is linked with many diet-related diseases including obesity (Brand-Miller et al., 2002; Roberts, 2000; Thornley, McRobbie, Eyles, Walker, & Simmons, 2008), diabetes (Jenkins et al., 2002; Wolever et al., 2008) and various cancers (Topping et al., 2008). Thus the digestibility of starch granules, both cooked and uncooked, is a high-priority research area. For nutritional purposes, starch was divided by Englyst (Englyst, Kingman, & Cummings, 1992) into three categories that depend on the rate and extent of its digestion: (1) rapidly digested starch; (2) slowly digested starch; and (3) resistant starch (RS). Slow hydrolysis of starch translates directly to slow uptake of glucose into the blood stream, and a reduction of insulin release rate from the pancreas, which appears to have health benefits (Roberts, 2000; Thornley et al., 2008). Starch that is undigested in the small intestine is fermented in the colon, producing short-chain fatty acids (predominately butyrate); this appears to protect colonic cells from DNA damage (Birkett & Brown, 2008; Haralampu, 2001).

Both slowly digested starch and RS are a consequence of the decrease in accessibility of the digestive enzymes to the starch polymer in solution (Chung, Lim, & Lim, 2006; Holm, Lundquist, Bjorck, Eliasson, & Asp, 1988). As a result, the extent of starch gelatinization is often measured by the amount of starch that is digested rapidly (Holm et al., 1988; Svihus, Uhlen, & Harstad, 2005). While food characteristics such as the presence of non-starch polysaccharides and starch retrogradation contribute to the rate and intestinal location of digestion of starch to glucose, it is also important to understand the processes involved in the digestion of starch granules in the absence of these complicating factors. The present study comprehensively followed the kinetics of product release from starch granules during their digestion with two selected hydrolytic enzymes. Its focus was to determine the 'best' kinetic model to describe the release of glucose from starch granules. Specifically the kinetic characterization of the release of products from starch granules considering their complex interactions in aqueous suspensions was analyzed.

The feed of domestic animals often includes uncooked starch granules, while human food usually includes gelatinized starch

Abbreviations: DSS, sodium 3-(trimethylsilyl)propane-1-sulfonate; NMR, nuclear magnetic resonance; RS, resistant starch.

* Corresponding author. Present address: Singapore Bioimaging Consortium, A*STAR, Helios, Singapore 138667, Singapore.
E-mail addresses: philip.kuchel@sydney.edu.au, philip_kuchel@sbis.a-star.edu.sg (P.W. Kuchel).

0144-8617/$ – see front matter © 2010 Elsevier Ltd. All rights reserved.
doi:10.1016/j.carbpol.2010.10.042

(wherein much of the primary granule structure is destroyed; however much of the secondary and tertiary structure remains (Mukerjea, Slocum, Mukerjea, & Robyt, 2006)); consumption of unprocessed starch is nevertheless significant for humans, e.g., in many breakfast cereals.

Several different hydrolytic enzymes within the digestive tract of animals and humans catalyze the breakdown of polymeric anhydroglucose (Fraser-Reid et al., 2001; Robyt, 1998). Two classes of enzyme catalyze the hydrolysis of starch to oligosaccharides and subsequently oligosaccharides to monosaccharides in the proximal sections of the gut; these are endohydrolases (Werner & Keilich, 1965) and exohydrolases (Akerberg, Zacchi, Torto, & Gorton, 2000). In the hydrolysis of polysaccharides, both types of enzyme operate sequentially to produce, ultimately, monosaccharides that are absorbed from the gut into the blood stream (Fig. 1). Carbohydrate endohydrolases cleave large polysaccharides to give smaller products; thus they operate at the early stages of digestion of a particular starch molecule. α-Amylase is an endohydrolase that is widely distributed in living organisms (only salivary and pancreatic amylase exist in humans). It is found in the digestive systems of mammals, and is also present in starch grains themselves. It catalyzes the hydrolysis of α (1,4) bonds, splitting a starch molecule into two smaller molecules.

Glucosidases release a monomer or dimer of glucose from the non-reducing end of oligosaccharides producing monomers that traverse cell membranes via specific membrane transport proteins, so they come into action in the terminal stages of polysaccharide digestion in humans. Glucoamylase (E.C. 3.2.1.3) (Kimura & Robyt, 1995; Kimura & Robyt, 1996a; Kimura & Robyt, 1996b) is an example of an exohydrolase that is produced by fungi and hydrolyzes glucose units from the end of starch or oligosaccharide molecules. Its action on the non-reducing end of polysaccharide oligomers, catalyzes not only the hydrolysis of α (1,4) linkages but to a lesser extent α (1,6) (branch) linkages, enabling the further degradation of non-linear oligosaccharides. In the small intestine, α (1,4) and α (1,6) glucosidases, secreted by the brush border cells that line the walls of the small intestine act only on oligomers that diffuse into this region after breakdown from larger starch entities by other enzymes.

It is of interest that starch-granule digestion can be characterized using similar mechanistic models in spite of which hydrolytic enzyme is used in the studies. During the present work it became evident that although enzyme characteristics (affinity for substrate and mechanism of reaction) determined the rate of digestion of solubilized substrate molecules, the restricted interaction that starch granules have with solvent water becomes rate determining for the hydrolytic reactions as digestion advances.

Although glucoamylase does not exist in the brush border of the mammalian small intestine, it is common practice to model the hydrolysis of starch granules by using this readily available and stable enzyme. Previous characterization of glucoamylase kinetics used less than ten time points over a 36 h time course (Kimura & Robyt, 1995; Kimura & Robyt, 1996a; Kimura & Robyt, 1996b). Deviations from Michaelis–Menten enzyme kinetics are only obvious with a much more detailed analysis of digestion time courses. In the present study we analysed each stage of granule digestion by recording glucose release over a large extent of reaction. The results provided evidence for the enzyme-kinetic models that then described each stage of granule digestion. Furthermore, in the present work we optimised a multistage kinetic model to describe completely the digestion of starch granules.

Rate data and kinetic analysis shed light on the mechanisms of various digestion processes. Michaelis–Menten kinetics (Cornish-Bowden & Hofmeyer, 2005; Kuchel & Ralston, 1992; Michaelis & Menten, 1913) describes, to a good level of approximation, the rate of oligosaccharide hydrolysis by glucoamylase (E.C. 3.2.1.3) as a function of the concentration of its various substrates. More complex models have been used for situations where the basic Michaelis–Menten equation is inconsistent with the data; one such case involves product inhibition (Kuchel & Ralston, 1992; Mulquiney & Kuchel, 2003). Various product-inhibition models, including competitive or non-competitive, have been used to describe the rate of digestion of starch granules, and oligosaccharides by glycohydrolases under many experimental conditions (Beltrame et al., 1987; Fujii & Kawamura, 1985; Kazaz, Desseaux, Marchis-Mouren, Prodanov, & Santimone, 1998; Lim, Lee, Shin, & Lim, 1999; Ohnishi, 1971; Wang, Zeng, Liu, & Yuan, 2006). Also, the adsorption of α-amylase (E.C. 3.2.1.1) onto the surface of crystalline starch is decreased by maltose and maltotriose (Leloup, Colonna, & Ring, 1991), while some studies have reported minimal inhibitory effects of products such as maltose and maltotriose (Moreira, Lenartovicz, & Peralta, 2004; Yoshikuni, 1988).

Product inhibition is a phenomenon that has not been broadly considered in nutrition, but it is of great importance: for example, whether or not a particular stage of digestion occurs rapidly is likely to affect satiety. Product inhibition of enzymes is normally a significant effect, as both substrate and inhibitor are structurally similar and therefore compete for binding in the active site. Competitive inhibition is usually most noticeable at low substrate concentrations as it is overcome at high substrate concentrations. Less commonly, uncompetitive inhibition occurs when the inhibitor only binds to a site that forms when the substrate is also bound to the enzyme (Kuchel & Ralston, 1992; Mulquiney & Kuchel, 2003); non-competitive inhibition occurs when an inhibitor binds to a site that is distinct from the substrate binding site; it brings about a change in the topology of the catalytic site and hence its turnover number.

The rate of starch digestion in the absence of effects such as retrogradation, or the presence of non-starch polysaccharides depends largely on two factors: (1) First, the molecular architecture or physicochemical characteristics of the starch granule, at all six levels of its structure (Ao et al., 2007; French & Knapp, 1950; Kerr, Cleveland, & Katzbeck, 1951; Kruger & Marchylo, 1985). Conclusions correlating the botanical origin, largely responsible for the architecture of the starch granule, with both *in vivo* and *in vitro* digestibility are well developed (Goni, Garcia-Alonso, & Saura-Calixto, 1997; Jenkins et al., 2002; Thompson, 2000). (2) Second, the hydration or physical conformation of starch in granules that are in aqueous solution. Heat and pressure used during the preparation of starch suspensions alter the rate of progression towards gelatinization, which increases the availability of starch chains to digestive enzymes (Chung et al., 2006; Chung, Yoo, & Lim, 2005; Eerlingen, Jacobs, & Delcour, 1994; Holm et al., 1988).

Structural properties of starch granule and molecules are complex and much research has been aimed at characterizing the glucose-release properties of the many different varieties (BeMiller & Whistler, 2009; Whistler, BeMiller, & Paschall, 1984). Many structural and functional properties of starch granules affect their rate of digestion by enzymes, and the overall extent of digestion (Dona, Pages, Gilbert, & Kuchel, 2010). Although the factors are too numerous to cover in depth here, they include: the chain and branch point distributions in the granule (Ao et al., 2007; French & Knapp, 1950; Kerr et al., 1951); the heating and shearing of the sample (Chung et al., 2006; Farhat et al., 2001; Fassler et al., 2006; Granfeldt, Eliasson, & Bjorck, 2000; Guraya, James, & Champagne, 2001; Holm et al., 1988; Shiotsubo, 1983); and the size distribution of the granules (Al-Rabadi, Gilbert, & Gidley, 2009; Kruger & Marchylo, 1985; Manelius, Qin, Avall, Andtfolk, & Bertoft, 1997; McLaren, 1963).

We present here analysis based on data from NMR spectroscopy that is more generally applied to identify solute molecules, even in complex, heterogeneous mixtures (Chapman, Beilharz, York, & Kuchel, 1982; Himmelreich, Drew, Serianni, & Kuchel, 1998;

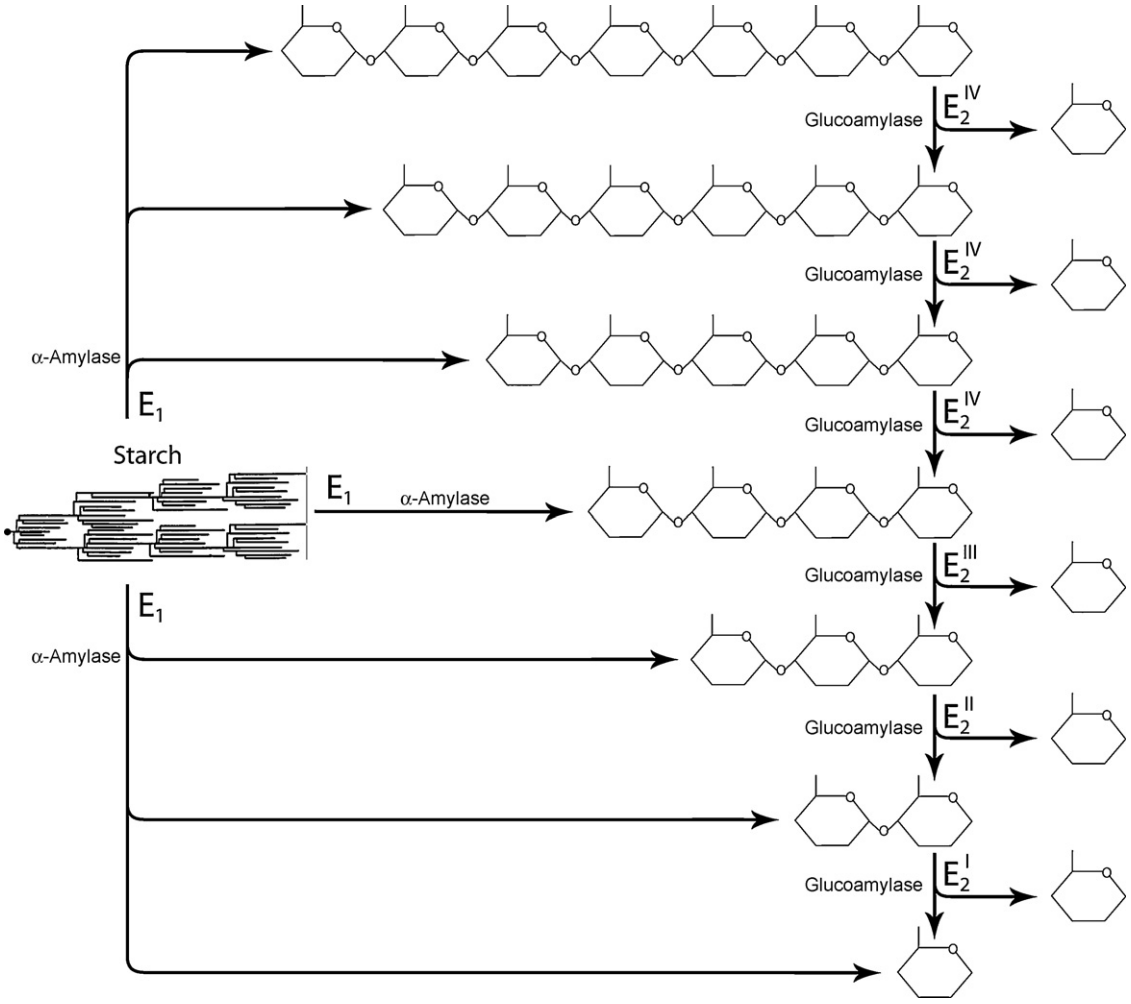

Fig. 1. Simplified pathway of saccharification that is followed by starch during its enzyme catalyzed hydrolysis. Each hexagonal ring represents a glucose unit, while E_1 and E_2 denote α-amylase and glucoamylase, respectively. The superscripts on each enzyme label refer to the significantly different values of the Michaelis–Menten constants that are necessary to describe the enzyme's action. The diagram does not include branched dextrin or oligosaccharides longer than maltoheptose that can be produced by α-amylase.

Kennett et al., 2005; King & Kuchel, 1984; King, Middlehurst, & Kuchel, 1986; Middlehurst et al., 1984; Raftos, Whillier, Chapman, & Kuchel, 2007; Whillier, Raftos, Chapman, & Kuchel, 2009). ^{1}H solution-state NMR has been used to monitor progress of physical and chemical processes in heterogeneous biological systems (Chapman et al., 1982; Himmelreich et al., 1998; Kennett et al., 2005; King & Kuchel, 1984; King et al., 1986; Middlehurst et al., 1984; Raftos et al., 2007; Whillier et al., 2009) including starch suspensions (Dona, Pages, Gilbert, Gaborieau, & Kuchel, 2009; Dona et al., 2007) provided that: (1) the nuclei monitored during the entirety of the reaction are in free solution; and (2) the heterogenous solution can be kept from settling (producing a vertical concentration gradient) during the time course (NMR spectroscopy usually only records signal from a small portion of the sample, within the volume sensed by the receiver coil, creating a bias in the measured concentration if particles of substrate settle in a sample). Although data for glucoamylase (E.C. 3.2.1.3) were obtained from free solution rather than in the surface environment of the brush border, it is posited that it is unlikely that this environment will affect the kinetics of the enzyme because solute uptake/accessibility has been optimized by natural selection, in this environment.

Various aspects of enzyme-catalyzed starch-granule digestion have been explored by many techniques over last 50 years. The techniques include: paper chromatography (Komaki, Matsuba, Okamoto, & Sato, 1959; Larner & McNickle, 1955); thin layer chromatography (Conway & Hood, 1976); high-performance liquid chromatography (Batey & Curtin, 1996; McCleary, 2007); and capillary electrophoresis (Noda et al., 2009; Singh, Isono, Srichuwong, Noda, & Nishinari, 2008; Soini & Novotny, 1999; Tueting, Albrecht, Volkert, & Mischnick, 2004). However, many novel features of granule digestion were able to be studied more directly by using ^{1}H NMR spectroscopy. The concentration of products in the sample can be more frequently measured by ^{1}H NMR, hence defining features of the product release curves were identified. Explaining these features led to the development of a two-stage model that describes granule digestion. Also, NMR analysis provided the advantage of measuring total oligosaccharide product without the need to inhibit enzymic action as the reaction occurred within the spectrometer. NMR analysis of granule digestion allowed digestion products to be differentiated from soluble starch chains, which could be further differentiated from insoluble portions of the granule at any stage during digestion. This led to a better understanding of aqueous solution-granule interactions during enzymic digestion.

The main questions addressed in the present study were: To what extent can the observed data on two isolated enzymic digestion steps for starch be fitted by solving the Michaelis–Menten differential equation without recourse to more complicated equa-

tions? If mechanistic elaborations are introduced into the models describing starch hydrolysis, to make them consistent with the known data, then what additional experimental evidence is necessary to justify these changes?

2. Experimental

2.1. Materials

Anhydrous α-D-glucose (AF404308; Ajax Finechems, NSW Australia) and D-maltose monohydrate (M5885, Sigma, St Louis, MO) were used for calibrating concentrations from ^{1}H NMR spectra in starch- and oligosaccharide-digestion experiments. For studies relating to starch digestion, α-amylase from *B. licheniformis* (E.C. 3.2.1.1; Megazyme, Wicklow, Ireland) supplied at a concentration of 3000 U mL^{-1} was added to rice starch (S-7260, Sigma, St Louis, MO) containing various amounts of glucose, maltose and maltotriose. Glucoamylase from *Aspergillus niger* (E.C. 3.2.1.3; A7095, Sigma, St Louis, MO) was obtained at a concentration of 300 U mL^{-1}, where a single unit of enzyme is defined as that amount which hydrolyzes the α (1,4) linkage of maltose at a rate of 1 μmol min^{-1}, at 25 °C. After appropriate dilution of either one of the enzymes was added to a starch suspension. The rates of hydrolysis of three types of starch were measured: purified rice starch (S-7260, Sigma); regular maize starch; and gelose 50 (Penford Food Ingredients Co., Centennial, CO). Both regular maize starch and gelose 50 are maize starch varieties with 27% and 50% amylose content (as reported by the manufacturer), respectively; both were pretreated with a "cocktail" of hydrolytic enzymes (Sopade & Gidley, 2009) including porcine pancreas α-amylase (A4268, Sigma), porcine mucosa pepsin (P7000, Sigma), porcine pancreas pancreatin (P7545, Sigma) and glucoamylase, which was halted after either 2 or 8 h. The rapid *in vitro* starch digestion assay was carried out as described previously (Sopade & Gidley, 2009).

2.2. Methods

2.2.1. ^{1}H Nuclear Magnetic Resonance

All NMR spectra were acquired on a Bruker Avance III spectrometer (Karlsruhe, Germany), equipped with a 9.4 T wide-bore vertical magnet (Oxford Instruments, Oxford, UK), operating at a radio frequency (RF) of 400.09 MHz for ^{1}H detection, using a 5-mm triple resonance inverse (TXI) probe. The probe temperature was set to 25 °C for all experiments. A Carr-Purcell-Meiboom-Gill (CPMG) pulse sequence was used with an echo time of 0.5 ms, and an echo pulse train of 100 repetitions (Meiboom & Gill, 1958); this pulse sequence decreases the broadness of the solvent-water peak because water has a short transverse relaxation time (Table 1). The pulse sequence also included a water pre-saturation pulse (power attenuation of the 100 W amplifier, 55 dB) during the relaxation delay to suppress the water peak even further. T_1 and T_2 values for signals from relevant carbohydrates were measured by using an inversion recovery and a CPMG pulse sequence, respectively (Table 1). The relaxation times were measured in various carbohydrates as the spin–lattice (T_1) and spin–spin (T_2) relaxation times can vary significantly with the degree of polymerization, concentration and immediate proton environment (i.e., intra- and inter-molecular environment) (Birch & Karim, 1992). The 90° pulse duration was ~11.5 μs; and the acquisition time (aq) and relaxation delay (d_1) were 8 s and 2 s, respectively. Each spectrum was derived from eight transients preceded by four dummy transients. Chemical shifts were calibrated using the resonance from sodium 3-(trimethylsilyl)propane-1-sulfonate (DSS, 178837, Sigma) at 0.000 ppm. Exponential line broadening of 1 Hz was used with no zero-filling. The data were recorded and processed using TOPSPIN 2.1 software (Bruker).

To calibrate ^{1}H NMR resonances for concentrations of α- and β-reducing ends of glucose molecules using the –$C_1\underline{H}$ resonance of glucose and oligoglucosides produced during hydrolysis, spectra of D-glucose standards were recorded at five concentrations from 10 to 100 mM prior to each set of experiments. The spectral intensities of the α- and β-reducing-ends from D-glucose standards were compared with the corresponding signals from other oligosaccharides of the same concentration; they all exhibited insignificant differences of total signal from their reducing-end hydrogen atoms. Digestion of oligosaccharides was also monitored by measuring the amount of residual α (1,4) link signal that was calibrated against five maltose standards of concentrations 10–100 mM. The T_1 and T_2 times were measured for relevant resonances in glucose and maltotetraose, revealing little difference (Table 1). Effects of magnetic pre-saturation of the population of water spins, or cross relaxation, on quantification of signals from oligosaccharides of various lengths, were found to be insignificant.

All digestion reactions were carried out in 40 mM sodium acetate buffer, at pH 5.3 (uncorrected pH meter reading) made up in D_2O, containing 10 mM DSS as an internal standard for the quantification of the concentration of hydrogen atoms on reducing-end glucose residues. Prior to enzyme addition, a ^{1}H NMR spectrum of each solution was recorded, and the integral of the –$C_1\underline{H}$ resonance of the α- and β-reducing ends was subtracted from the signal recorded during the time course. Enzyme solution (0.3 U mL^{-1}) was added to the oligosaccharide solutions of concentrations (mM) ~5, 10, 20, 40, and 100. The delay between beginning the enzymic reaction and recording a ^{1}H NMR spectrum was precisely timed (~2 min); then up to 500 ^{1}H NMR spectra (~2 min each) were acquired sequentially.

2.2.2. Preparation of slowly digested starch

The rice-starch granules used to study the kinetics of rapidly digested starch were not pre-treated in any way. Starch used to study the kinetics of slowly digested starch was first treated with enzyme to remove the rapidly released glucose. In the case of rice starch, 0.4 g of starch was suspended in 10 mM acetate buffer (20 mL, pH 5.3) with stirring. 2 U mL^{-1} of α-amylase was added and the reaction mixture was incubated for 30 min at 25 °C (as this was well after the completion of the rapidly digested starch stage); at the end of the incubation period enzyme and oligosaccharide products were removed from the starch by filtering the sample through a Microcon centrifugal filter (42413, regenerated cellulose, 100 kDa; Micon, Bedford, MA) and washing three times with MilliQ water. The starch granules remaining were dried overnight at 40 °C and used for the kinetic characterization of slowly digested starch.

The study of the rapidly digested stage of maize starch samples (regular maize starch and Gelose 50) was carried out using untreated samples. Two slowly digested starch samples of each maize starch were also created by passing samples of each through a rigorous process that mimics *in vivo* digestion (Sopade & Gidley, 2009); the method uses a "cocktail" of enzymes (Section 2.1) at 37 °C and pH 2.0–7.0. After 2 and 8 h the enzyme activity was halted using acetone, and then the starch samples were freeze dried. These samples were used to study the different stages of digestion of maize starch slowly digested starch. The samples are referred to below by the abbreviations RMS2HR, RMS8HR, G502HR, and G508HR.

2.2.3. Fitting kinetic data

The enzyme-catalyzed hydrolysis of the α (1,4) linkage in maltose can be described by the conventional Michaelis–Menten reaction scheme:

$$\text{Maltose} + \text{Enzyme} \overset{\text{glucoamylase}}{\underset{k_{-1}}{\overset{k_1}{\rightleftharpoons}}} \text{E-Maltose} \xrightarrow{k_2} 2\text{D-Glucose} + \text{Enzyme} \quad (1)$$

Table 1
T_1 and T_2 NMR relaxation times for various carbohydrates.

Water	T_1 relaxation time (s)			T_2 relaxation time (s)		
	0.10 ± 0.02[a]			0.11 ± 0.02		
	α(1,4)-C$_1$H	β(1,4)-C$_1$H	α(1,4) link-C$_1$H	α(1,4)-C$_1$H	β (1,4)-C$_1$H	α(1,4) link-C$_1$H
Glucose	3.10 ± 0.12	1.78 ± 0.07	N/A	2.25 ± 0.10	0.28 ± 0.05	N/A
Maltotetraose	2.20 ± 0.09	1.45 ± 0.05	1.13 ± 0.05	1.99 ± 0.12	0.50 ± 0.07	0.99 ± 0.09
Starch	2.30 ± 0.15		1.30 ± 0.18	1.07 ± 0.12		0.41 ± 0.12

[a] Denotes ± standard deviation; N/A means not applicable.

where E-Maltose is the enzyme–substrate complex, and k_1, k_{-1}, and k_2 are unitary rate constants. Unlike polymers of dehydroglucose, such as starch and cellulose, short-chain oligosaccharides have high solubility in water and therefore are easily accessed by enzymes in solution. Hence the kinetics of hydrolysis can be described by the Michaelis–Menten differential equation (Eq. (2)),

$$\frac{d[P]}{dt} = \frac{V_{max}[S]}{K_m + [S]}, \tag{2}$$

where $V_{max} = k_2[E]_0$ is the maximum velocity of the reaction, [P] is the concentration of the glucose product, and K_m is the Michaelis constant (Eq. (3)) described in terms of the unitary rate constants (see Eq. (1)):

$$K_m = \frac{k_{-1} + k_2}{k_1}. \tag{3}$$

Michaelis–Menten constants were estimated for a range of maltose concentrations by minimizing the sum of the squares of the residuals between the data and numerically integrated Eq. (2) using a program written in *Mathematica* (Mulquiney & Kuchel, 2003).

Having estimated the values of the kinetic parameters (K_m and V_{max}) for the hydrolysis of maltose, the hydrolysis of maltotriose into glucose units was able to be completely characterized using the kinetic parameters previously estimated for maltose hydrolysis.

In the past, digestion kinetics have been analyzed using double reciprocal plots such as Lineweaver–Burk or Hanes–Woolf plots (Nitta, Kunikata, & Watanabe, 1979). Although this analysis avoids solving the Michaelis Menten differential equation, the reciprocal plots have large systematic errors. Fitting the transformation of a nonlinear equation to experimental data distorts the errors in the measured variables, subsequently impacting on the veracity of estimates of the kinetic parameters. Even more statistically robust is the direct linear plot method of Eisenthal and Cornish Bowden (Eisenthal & Cornish-Bowden, 1974). Recent advances in computation allow for numerical integration of differential equations and to use these solutions to fit time courses of data, to estimate parameters. This approach was used in the present study and it afforded small deviations in regression analysis of digestion time courses.

The kinetics of hydrolysis were recorded by measuring the change in either: (1) the ^{1}H NMR α (1,4) link resonance (5.4 ppm); or (2) the sum of the normalized α- and β-reducing-end resonance (5.2 and 4.7 ppm, respectively) for all linear oligosaccharides of glucose, up to maltoheptaose, thus yielding estimates of the K_m and V_{max} values for glucoamylase (E.C. 3.2.1.3; Fig. 2). Fixing known parameters ensured that a maximum of two parameters (K_m and V_{max}) were floated during least-squares regression analysis, for any subsequent length of oligosaccharide used.

Various enzyme-kinetic models can describe the digestion of starch to correlate 'digestibility' of starch granules with their physical properties. The majority of kinetic models for hydrolytic enzymes such as α-amylases or glucoamylases are based on the mechanism shown in Scheme 4:

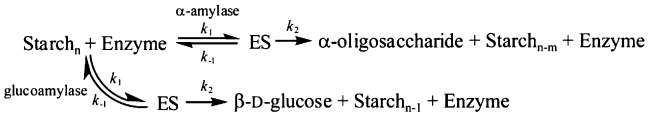

(4)

where Starch$_n$ denotes a starch molecule with n glucose units, ES is the enzyme–starch complex, and α-oligosaccharide consists of m glucose units. The unitary rate constants, k_1, k_{-1} and k_2 characterize the rate of each respective step in the reaction scheme.

The analytical solution of the Michaelis–Menten equation is nonlinear and implicit with respect to the substrate concentration. An explicit form of the integrated equation is often approximated by introducing reasonable constraints, causing only one of the terms on the right-hand side to dictate its value. Thus, if $K_m \ll [S]_0$, then the solution of the differential equation becomes a simple zero-order decay where the rate of reaction is independent of the extent of reaction. If the opposite occurs, $[S]_0 \ll K_m$, then the Michaelis–Menten equation reduces to a first order differential rate equation (Eq. (5));

$$\frac{d[P]}{dt} \approx \frac{V_{max}[S]}{k_m}, \tag{5}$$

which when solved, describes the depletion of the substrate via a single exponential function.

Competitive inhibition occurs when the binding of the inhibitor to the enzyme prevents binding to the substrate, and vice versa. As well as being used to explain the kinetics of many enzyme–substrate systems, the competitive inhibition model has also been used to describe product inhibition of glucoamylase (E.C. 3.2.1.3) by glucose (Fujii & Kawamura, 1985; Lim et al., 1999; Wang et al., 2006) (Eq. (6)),

$$\frac{d[P]}{dt} = \frac{V_{max}[S]}{K_m(1 + ([P]/K_i)) + [S]}, \tag{6}$$

where K_i is the product-inhibition constant. The double reciprocal of the competitive inhibition equation yields a value for when the reciprocal of the initial velocity is plotted against the initial inhibitor concentration. This approach was used in the present study to measure the (slight) inhibition of α-amylase by maltose.

In the early stages of starch-granule digestion, ^{1}H NMR signals arise from the non-reducing ends of glucose residues that are mobile in the aqueous medium. These signals decay as the polymer chains are hydrolyzed into residual or core products that do not have residues with the same mobility and hence NMR visibility. Thus in the early stages of the reaction the additional signals lead to an overestimation (background) of the concentration of the products. Hence, when modeling the time course for data analysis an additional differential equation with a fast decay constant

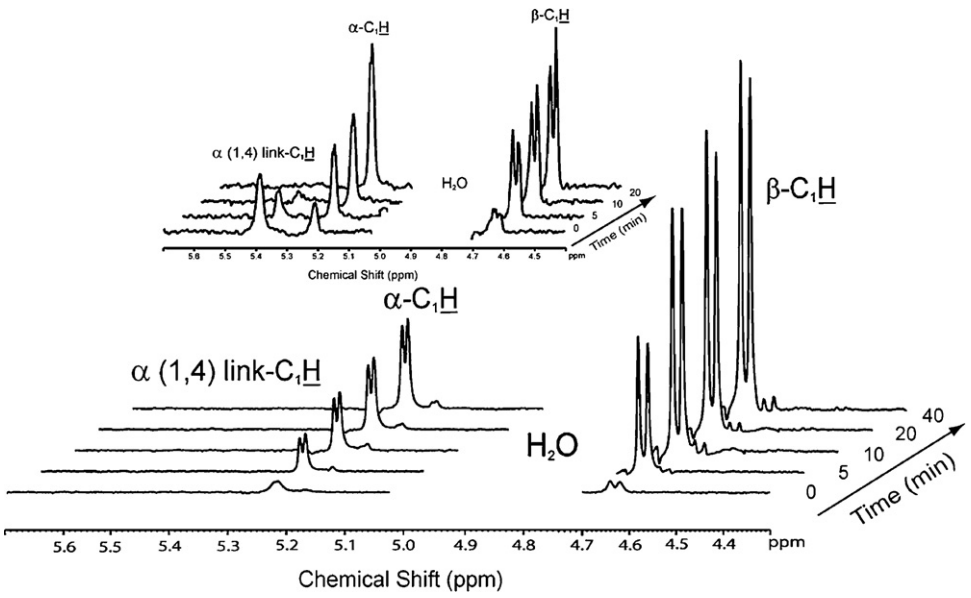

Fig. 2. Time evolution of ^{1}H NMR (400.13 MHz) spectra showing the digestion of slowly digested starch with glucoamylase, at pH 5.3 and 25 °C. The signal from HDO (D_2O-water mixture) normally appearing at 4.9 ppm was absent due to the pre-saturating CPMG pulse sequence used (Section 2). *Inset:* Time evolution of ^{1}H NMR spectra showing the digestion of rapidly digested starch with glucoamylase, at pH 5.3 and 25 °C.

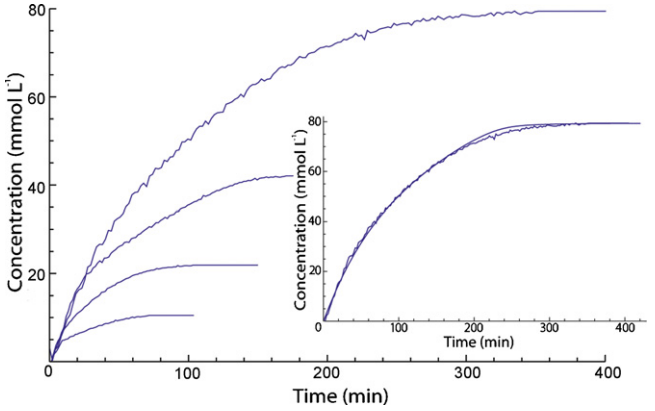

Fig. 3. Concentration of α (1,4) link-C_1H hydrolyzed during digestion of maltotriose (5, 10, 20, and 40 mM) with the addition of 1.2 U mL^{-1} of glucoamylase. *Inset:* Nonlinear regression of the numerically integrated Michaelis–Menten differential equation (Eq. (2)) onto digestion data, from 40 mM maltotriose.

was included to account for this slightly irregular early stage of the timecourse (see Fig. 8). Its inclusion brought about only a small change (a few %) in the estimates of Michaelis–Menten parameters (see Supplementary Information).

3. Results and discussion

3.1. Oligosaccharide digestion

Accurate estimation of the Michaelis–Menten parameters of glucoamylase from *Aspergillus niger* (E.C. 3.2.1.3) for the cleavage of oligosaccharides up to a length of seven glucose units was performed. By first measuring the kinetic parameter values for maltose, these were then used when estimating the kinetic parameters for maltotriose; and so forth to estimate the Michaelis–Menten parameters for all oligosaccharides through to maltoheptaose.

The ^{1}H NMR-recorded enzymic hydrolysis of maltotriose by glucoamylase clearly showed multiple stages over time (Fig. 3). The initial rate of cleavage of the α (1,4) linkages of maltose was significantly less than that in maltotriose at the same enzyme concentration. This trend continued for digestion of the longer oligosaccharides. Digestions of longer oligosaccharides were able to be fitted using separate Michaelis–Menten steps as shown for maltotriose (Fig. 3 *inset*). Estimates of both the V_{max}, and K_m significantly increased for the first three linear oligosaccharides of glucose (Table 2). In addition, the ratio between the maximum velocity of hydrolysis of maltotriose to maltose was ~4; this value is in close agreement with a previous study on oligosaccharide digestion using three isoforms of glucoamylase (Miah & Ueda, 1977).

Studies of glucoamylase by modified structure-based sequence alignment, site-directed mutagenesis, and single anomalous dispersion phasing, reveals two binding sites, although kinetic analysis of glucoamylase conflicts with substrate-binding-site structural studies (Chou, Pai, Liu, Hsiung, & Chang, 2006; Heymann, Breitmeier, & Guenther, 1995; Miah & Ueda, 1977; Sim, Quezada-Calvillo, Sterchi, Nichols, & Rose, 2008). In the present study, estimates of K_m and V_{max} reached limiting values upon digestion of oligosaccharides longer than maltotetraose, consistent with the notion of multiple substrate-binding-sites arrived at in the structural studies (Chou et al., 2006; Heymann et al., 1995; Miah & Ueda, 1977; Sim et al., 2008).

The structural studies also show that glucoamylase contains two homologous catalytic domains that differ in substrate specificities, despite their close structural similarity (Sim et al., 2008): an *N*-terminal subunit and a *C*-terminal subunit. The active site of the *N*-terminal subunit contains only two glucose-residue subsites, thus not explaining the different enzymic action on oligosaccha-

Table 2
Estimated V_{max} and K_m values for the hydrolysis of the first α (1,4) link in oligosaccharide chains of various lengths with 0.3 U mL^{-1} of glucoamylase.

Oligosaccharide	Michaelis constant (K_m) (mM)	Maximum velocity (V_{max}) $10^2 \times (\pm$ mM s^{-1})
Maltose	2.5 ± 0.2	0.23 ± 0.01
Maltotriose	5.3 ± 0.3	1.15 ± 0.05
Maltotetraose	8.8 ± 0.5	2.73 ± 0.08
Maltopentaose	7.3 ± 0.7	2.92 ± 0.13
Maltohexaose	6.9 ± 1.1	2.82 ± 0.21
Maltoheptaose	6.5 ± 1.2	2.74 ± 0.35

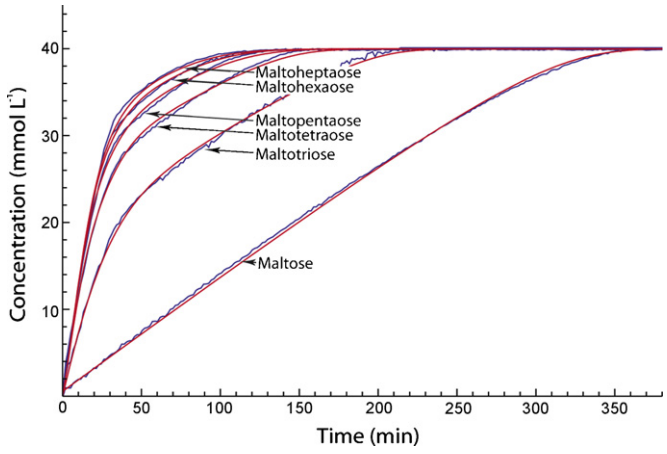

Fig. 4. The concentration of α (1,4) link-$C_1\underline{H}$ hydrolyzed (*blue*) during digestion of linear oligosaccharides of anhydroglucose residues after the addition of 0.3 U mL^{-1} of glucoamylase at 25 °C, and simulated data using the estimates of kinetic constants given in Table 2 (*red*). The initial concentration of each oligosaccharide was calculated so that it would yield exactly 40 mM of α (1,4) link-$C_1\underline{H}$ bonds. (For interpretation of the references to color in this figure legend, the reader is referred to the web version of the article.)

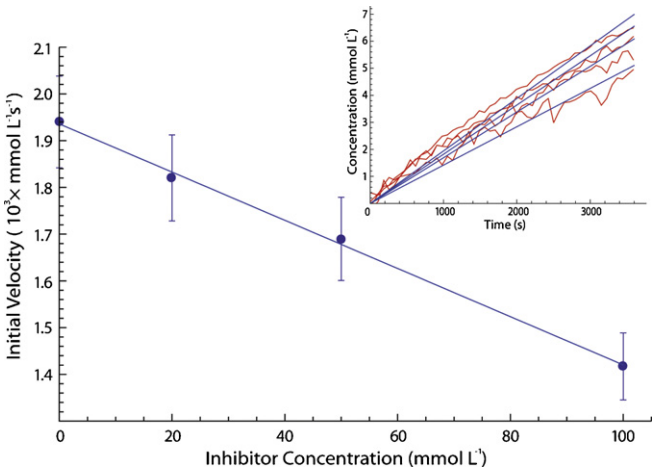

Fig. 5. Initial reaction velocity of α-amylase (15 U mL^{-1}) hydrolysis of maltopentaose (20 mM) as the concentration of maltose (0, 20, 50, and 100 mM) was increased, yielding an estimate of $K_i = (2.7 \pm 0.4) \times 10^2$ mM. *Inset:* Linear fits (*blue*) to digestion data (*red*) during the initial stages of α-amylase digestion of maltopentaose with various maltose (acting as an inhibitor) concentrations. (For interpretation of the references to color in this figure legend, the reader is referred to the web version of the article.)

rides from maltose to maltotetraose. However, the *C*-terminal active site is proposed to have four glucose-residue-binding subsites with additional interacting residues; this accounts for the increase in binding affinity up to maltotetraose (Sim et al., 2008) (Fig. 4 and Supplementary Material).

The presence of competitive product inhibition of glucoamylase has been inferred by fitting data in a Lineweaver–Burk plot (Fujii & Kawamura, 1985). However, such plots skew experimental errors (inherent in all double reciprocal plots), so the estimate of K_m here was made by nonlinear least squares regression analysis of the Michaelis–Menten equation onto the untransformed data. No correlation was found between the initial concentration of glucose and the estimated apparent K_m for maltose hydrolysis with glucoamylase. Furthermore, the classical Michaelis–Menten equation (Eq. (2)), when integrated numerically, very accurately fitted experimental time courses, even when there were large initial concentrations of D-glucose present (the product of the reaction). This showed that product-inhibition models were not necessary to describe the kinetics of glucoamylase from *Aspergillus niger* (E.C. 3.2.1.3) with oligosaccharide substrates.

The influence of small oligosaccharides on the kinetics of α-amylase from *B. licheniformis* (E.C. 3.2.1.1) was also investigated, as product inhibition is often used to explain the deviation from Michaelis–Menten kinetics of similar enzymes during starch digestion. Various concentrations (0–500 mM) of maltose (the most common product of α-amylase hydrolysis) were added to starch suspensions (1.5 %, w/w) in these experiments. No significant effect on the rate of hydrolysis was seen upon overlaying the data obtained from hydrolysis of starch granules in the presence of various concentrations of maltose (see Supplementary Material). Although a mechanism-based rate equation was not used to analyze the inhibited hydrolysis of starch granules, as a simple one stage model cannot accurately describe granule hydrolysis (Dona et al., 2009), the digestion rate of starch granules did not appear to be significantly affected by maltose.

It was apparent that the kinetics of starch digestion by α-amylase was not significantly affected by the presence of product; to explore this further, a study of α-amylase action on oligosaccharides was performed. The enzyme was seen to act relatively rapidly on all oligosaccharides larger than maltose. However, the action of α-amylase on oligosaccharides shorter than its binding site, which is five sub-sites long (Yoon & Robyt, 2003), was far less rapid than its action on starch granules. Product inhibition of α-amylase by maltose in digestion mixtures was apparent when the substrate was a short oligosaccharide. Experiments on the digestion of maltotetraose with α-amylase showed a significant decrease in initial velocity as the initial concentration of maltose was increased (Fig. 5). Under experimental conditions when the apparent K_m of the product-inhibition model is much larger than the substrate concentration (i.e., $K_m(1 + [P]/K_i) \gg [S]$), the rate equation can be linearized (Eq. (7)):

$$\frac{1}{(d[P]/dt_0)} = \frac{K_m}{V_{max}[S]} + \frac{K_m[P]}{K_i V_{max}[S]} \quad (7)$$

Upon plotting the reciprocal of the initial reaction velocity against the inhibitor concentration, the data were fitted with a straight line that yielded an estimate of the product inhibition constant ($K_i = (2.7 \pm 0.4) \times 10^2$ mM) and K_m/V_{max}. While maltose was seen to inhibit α-amylase (weakly), the extent of inhibition was insignificant in the digestion of starch granules under almost all circumstances.

3.2. Starch digestion

Before enzyme addition, the intensity of the α (1,4) link ^{1}H NMR resonance is related to the amount of free, solvated starch that is accessible to enzymes. Before hydrolysis via glucoamylase from *Aspergillus niger* (E.C. 3.2.1.3), untreated starch has a large α (1,4) link resonance, so a (small) portion of the starch granule was evidently free in solution (Fig. 2). The signal decreased during digestion as glucoamylase cleaved the terminal α (1,4) linkages. Starch previously treated with the enzyme (slowly digested starch) has essentially no initial ^{1}H NMR resonance corresponding to the α (1,4) link hydrogen atoms (Fig. 2 *inset*). Therefore at the end of the rapidly digested stage of the reaction, the solvated starch chains had been completely hydrolyzed. Furthermore, the depletion of the α (1,4) link ^{1}H NMR resonance during the digestion reaction with untreated starch had a time course that coincided with that around the deviation from rapidly digested starch to slowly digested starch (Dona et al., 2009). This suggests that the portion of starch granules initially solvated contributed to the generation of reducing sugars from rapidly digested starch. The ^{1}H NMR signal from α (1,6) linkages was not monitored in the present work as it is not well resolved

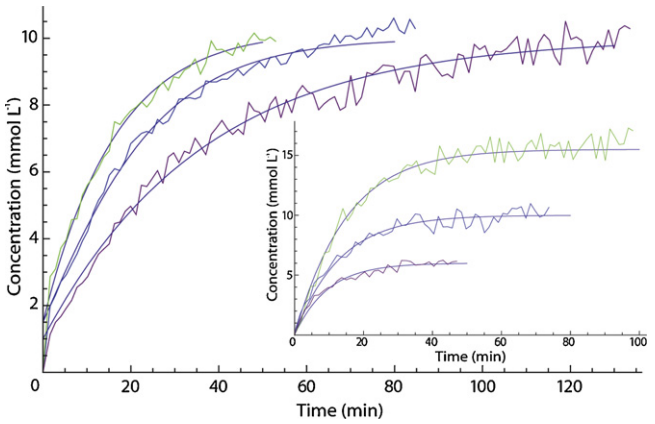

Fig. 6. Prediction of glucose production from 40 mg mL^{-1} rapidly digested starch by the Michaelis–Menten rate equation, for glucoamylase: 1.2 U mL^{-1} *green*; 0.6 U mL^{-1}, *blue*; 0.3 U mL^{-1}, *purple*; at 25 °C and pH 5.3. The Michaelis constant, K_m, for the simulated data was 1.95 ± 0.33 mmol L^{-1}, and the maximum velocities, V_{max}, for each were: $(5.2 \pm 0.6) \times 10^{-2}$ mM s^{-1}, *green*; $(2.7 \pm 0.2) \times 10^{-2}$ mM s^{-1}, *blue*; $(1.5 \pm 0.2) \times 10^{-2}$ mM s^{-1}, *purple*. *Inset:* The Michaelis–Menten approximation-prediction of glucose production from rapidly digested starch: 80 mg mL^{-1}, *green*; 40 mg mL^{-1}, *blue*; 20 mg mL^{-1}, *purple*; with glucoamylase (0.6 U mL^{-1}), and $K_m = 1.95 \pm 0.33$ mM, and $V_{max} = (2.7 \pm 0.2) \times 10^{-2}$ mM s^{-1}. (For interpretation of the references to color in this figure legend, the reader is referred to the web version of the article.)

in the spectra; and in any case it was irrelevant for α-amylase digestion and it only had very minor consequences for the fitting of data from glucoamylase digestions.

The digestion of starch by either glucoamylase or α-amylase showed very similarly shaped kinetic time courses of product formation during starch digestion (Fig. 8 and Supplementary Material). ^{1}H NMR signals from solvated α (1,4) linkages could not be distinguished from those due to oligosaccharide products from α-amylase. Glucoamylase was therefore used during incubations to study the change in solvated starch and its effects on the kinetics of digestion. Our results indicate that the stage during starch digestion when the reaction becomes significantly slower (slowly digested starch) corresponds to the state of the granules when they have been stripped of their solvated chains. Concomitantly, the solubility of starch granules largely determines when digestion becomes significantly slower.

3.2.1. Rapidly digested starch

Although several different enzyme-kinetic models have been used to describe the production of reducing sugar during starch digestion, an exponential model can often accurately describe time courses (Al-Rabadi et al., 2009; Apar & Ozbek, 2007; Frei, Siddhuraju, & Becker, 2003; Goni et al., 1997; Hill, Macdonald, & Lang, 1997; Komolprasert & Ofoli, 1991; Wang et al., 2006). Such time courses, analyzed by ^{1}H NMR spectroscopy, verified the ability of an exponential model to describe the data (Supplementary Material). ^{1}H NMR spectroscopy has the advantage over other techniques used to observe starch digestion of being able to take very regular time points to monitor the release of reducing sugars. Deviations from an exponential model are made evident during the stage of rapidly digested starch upon linearization of the digestion data using a log-linear plot. In fact, the kinetics of glucose production during the stage of rapidly digested starch can very accurately be described by the numerical integration of the classical Michaelis–Menten equation (Eq. (2), Fig. 6). The initial period of product release by hydrolytic enzymes from starch is relatively short-lived (more correctly termed a 'small extent of the total reaction'); therefore during this stage, the product inhibition of maltose on α-amylase was insignificant and did not need to be considered further.

Parameter values estimated by fitting the numerically integrated Michaelis–Menten differential equation to the rapidly digested starch data yield V_{max} values that were directly proportional to the concentration of the enzyme, as expected for a Michaelis–Menten enzyme (Fig. 6). Furthermore, the amount of starch digested during this period was directly proportional to the amount of substrate (starch) present (Fig. 6 *inset*). The K_m estimates displayed no significant change with enzyme or initial substrate concentration, again as expected for a Michaelis–Menten enzyme. Therefore, this experimental evidence supported the use of Michaelis–Menten kinetics to describe the initial stages of starch digestion (rapidly digested starch). Making the assumption that starch-chain residues are all longer than the binding site subunits of the enzyme, a single Michaelis–Menten equation was used to describe the rapidly digested starch stage.

This being the case, the initial rate of reducing sugar produced *in vivo* should depend primarily on the amount of enzyme produced in glandular secretions. In humans, the amount of α-amylase in salivary and pancreatic secretions varies in response to factors such as insulin concentration and pancreatic tissue depletion, which concomitantly determine the initial rate of starch digestion (Fried, Abramson, & Meyer, 1987; Gubern, Canalias, & Gella, 1995). Further, the amount of oligosaccharide produced during the rapidly digested starch stage depends only on the amount and type of carbohydrate ingested and not strongly on the enzyme-kinetic parameter values.

3.2.2. Slowly digested starch

Following the hydrolysis of the outer, fully hydrated branches of the starch granule, the digestion becomes impeded (French & Knapp, 1950; Kerr et al., 1951). A major portion of an untreated starch granule is insoluble in water, thus invalidating the basic assumptions concerning substrate accessibility required of Michaelis–Menten enzyme kinetics. Hence the rate of product formation is significantly reduced during the slowly digested starch stage; this is due to the putative inaccessibility of the substrate to the enzyme. There is considerable evidence that enzyme mediated release of reducing sugar during the slowly digested starch stage is describable by an exponential expression (Al-Rabadi et al., 2009; Apar & Ozbek, 2007; Fried et al., 1987; Goni et al., 1997; Hill et al., 1997; Wang et al., 2006). However, classical Michaelis–Menten kinetics has also been used to describe the kinetics of digestion of starch during the slowly digested starch stage (Akerberg et al., 2000; Amato et al., 2004; Dona et al., 2009; Heitmann, Wenzig, & Mersmann, 1997; Nitta et al., 1979; Park & Rollings, 1995). Product- or substrate-inhibition models have also been used to describe the entirety of the time courses of hydrolysis of starch granules (Fujii & Kawamura, 1985; Pastrana, Gonzalez, Miron, & Murado, 1998). The factors controlling the rate of reducing sugar released during the slowly digested starch stage were also explored using starch previously treated with glycohydrolytic enzymes (Section 2).

It was found here that varying the concentration of α-amylase with the insoluble core of starch granules did not significantly change the rate of digestion. In other words, at a given concentration of slowly digested starch, the digestion was independent of the concentration of α-amylase present; this is contradictory to the Michaelis–Menten enzyme-kinetic description (Supplementary Material). In contrast, in experiments where the concentration of enzyme was kept constant and the starch concentration was increased, the initial rate of product formation increased. The initial rate of oligosaccharide production was directly proportional to the concentration of substrate (Fig. 7). Normalizing the concentration of oligosaccharide during the time course using the reducing sugar concentration at long ("infinite") time (the initial glucose equivalent concentration of starch) and linearizing the data according to the method of Goni et al. (Goni et al., 1997) yielded similar estimates

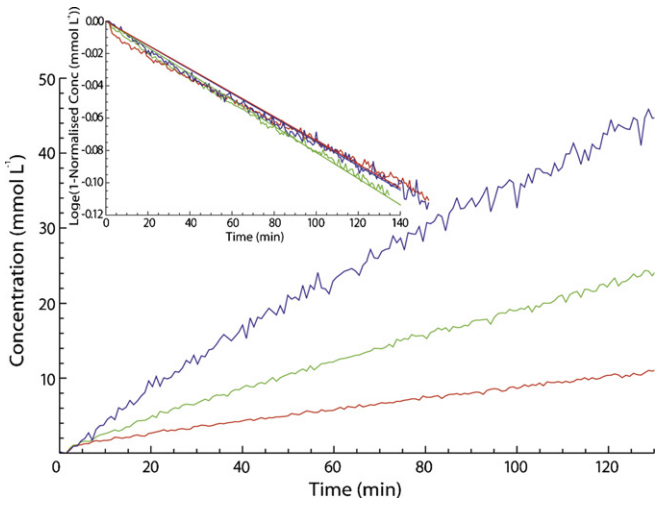

Fig. 7. Concentration of oligosaccharide produced during the digestion of slowly digested starch: 80 mg mL^{-1}, *blue*; 40 mg mL^{-1}, *green*; 20 mg mL^{-1}, *red*; with α-amylase (0.6 U mL^{-1}) at 25 °C and pH 5.3. *Inset:* The logarithmic plots were normalized to the initial slowly digested starch concentration and used the same exponential-decay rate constant, $k = V_{max}/K_m = (7.6 \pm 0.3)^{-4}$ s^{-1}. (For interpretation of the references to color in this figure legend, the reader is referred to the web version of the article.)

for the exponential rate constant of the reaction (Fig. 7 *inset*).

During the slowly digested starch stage of the reaction, the rate at which the enzyme–substrate complex was formed (k_1 [S]) was significantly decreased, concomitantly increasing the value of K_m. As explained above, the Michaelis–Menten equation reduces to a first-order differential rate equation when $[S]_0 \ll K_m$ (Eq. (5)). The rate of product formation is then described by a single exponential in which the first-order rate constant is equal to V_{max}/K_m. Experimental data from enzyme-mediated digestion of various concentrations of slowly digested starch provided evidence for using the single exponential to estimate the rate constant which was independent of substrate concentration (Fig. 7 *inset*). Furthermore, the initial rate of oligosaccharide production during the slowly digested starch stage of the reaction was directly proportional to the substrate concentration; and it was independent of enzyme concentration, as predicted by the exponential limit of a Michaelis–Menten enzyme (Eq. (5)). The extent to which the slowly digested starch had been degraded also did not affect its rate of digestion, only its concentration; this was consistent with the exponential model (Supplementary Material).

Each stage of starch digestion was analyzed with each enzyme (α-amylase and glucoamylase) individually. The kinetics of product formation was similar for each enzyme separately; thus the rate of product formation was largely determined by the structure of the starch granule. Also similar kinetics during the slowly digested starch stage of the reaction were observed when either enzyme was used individually.

By considering the results obtained for the rapidly digested starch and slowly digested starch stages of the reaction, a two-stage (but readily generalizable to more) model was implemented in the description of the time course of maize-starch digestion. This model consists of two differential equations that describe the release of reducing sugar from the commencement of starch digestion (Fig. 8). The concentration of rapidly digested starch was empirically (by trial and error iterations of simulations of the system) set to 25% of the original glucose-residue-equivalent starch concentration. The kinetics of this stage were fitted by a classical integrated Michaelis–Menten rate equation (Eq. (2)). The concentration of slowly digested starch in the rice starch samples was empirically (as for the maize starch) set to 60% of the original glucose-residue-equivalent starch concentration. This stage was represented in the

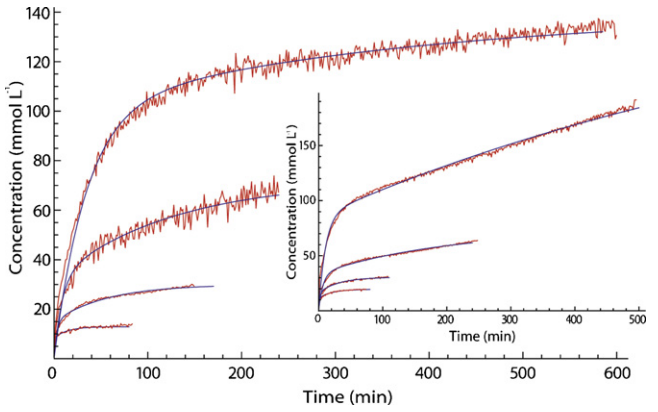

Fig. 8. Concentration of glucose produced during the digestion of untreated regular maize starch (5, 10, 20, 40 mg mL^{-1}) with glucoamylase (1.2 U mL^{-1}) at 25 °C and pH 5.3 (*red*). The two-stage model (see text) was used to estimate the rate constants for the production of glucose (*blue*). ($K_{mRDS} = 5.1 \pm 0.9$ mmol L^{-1}, $K_{mSDS} = 64.8 \pm 7.9$ mM, $V_{max} = (1.8 \pm 0.3) \times 10^{-2}$ mM s^{-1}.) *Inset:* Digestion of gelose 50 under the same conditions as regular maize starch. ($K_{mRDS} = (1.4 \pm 0.3) \times 10^{-1}$ mM, $K_{mSDS} = 4.8 \pm 1.3$ mM, $V_{max} = (1.4 \pm 0.3) \times 10^{-2}$ mM s^{-1}.) (For interpretation of the references to color in this figure legend, the reader is referred to the web version of the article.)

model by an exponential function where the rate constant was equal to V_{max}/K_{mSDS}. Three parameters were fitted to the experimental data using numerical integration; V_{max} was forced to have the same value during both stages, and there were two Michaelis constants K_{mRDS} and K_{mSDS}. The K_m values estimated for slowly digested starch were on average 13 times greater (lower apparent affinity) than those applicable in the rapidly digested starch stage. The rapid increase in the value of K_m for this system indicated why exponential models have been found to describe well the major extent of time courses of digestion of granular starch digestion.

Changing the amylose content of a starch substrate did not affect the ability of our multistage model to predict the forms of time courses of digestion; the changed composition however did affect the estimated parameter values (Fig. 8 *inset*). Both K_m values found for each stage during the digestion of 'gelose 50' were significantly less in comparison with the regular maize starch with lower amylose content. The ratio between the K_m for the slowly digested starch stage of the reaction and the rapidly digested starch stage, was far larger for 'gelose 50' (>30). The larger shift in the K_m value from rapidly digested starch to slowly digested starch was evident from the rapid change in slope in the digestion time course (Fig. 8). The higher amylose content was likely to have been responsible for the larger variation in digestion rates between the stages, as there were less reducing ends available for the hydrolytic enzyme to act on.

4. Conclusions

The complex structure of starch granules has a major effect on the rate of release of oligosaccharides and glucose during digestion by at least the two glycohydrolytic enzymes studied in the present work. Although many physical properties can affect the rate of product release, the kinetics of starch digestion could still be described by reasonably simple differential equations. Evidence provided here shows that initially the surface chains, which are hydrated, were hydrolyzed in a time course that was as predicted by Michaelis–Menten enzyme kinetics (rapidly digested starch). Subsequent to the rapidly digested starch stage of the reaction, the rate of digestion significantly decreased and this was surmised to be due to the insoluble core of the granule being reached. During the slowly digested starch stage of the reaction the time course was accurately described by a first order differential rate equation, supposedly due to the rate-determining step becoming the

penetration of the enzyme molecules into the insoluble portion of the granules. Both the Michaelis–Menten equation and a simple exponential function have been used in the past to describe starch digestion during the slowly digested starch stage of the reaction. We conclude here that both models describe the data acceptably well, considering that the Michaelis–Menten equation simplifies to an exponential function as the substrate concentration becomes small relative to K_m. The experimentally measured rate of release of reducing sugar (oligosaccharides and glucose) is deemed to be proportional to the surface area of substrate at a later stage of the reaction, as is consistent with our kinetic model. Assuming the surface area of starch to be proportional to its concentration, the rate of digestion in the slowly digested starch stage is predicted to be dependent on the concentration of starch.

Phenomenological expressions describing various forms of product inhibition of enzymes do not accurately describe the action of the two main hydrolytic enzymes involved in starch digestion. α-Amylase is inhibited by maltose although the effect only becomes significant when products of starch digestion accumulate massively.

In the degradation of starch granules, the digestion of oligosaccharide products up to a length of seven glucose units with either α-amylase (E.C. 3.2.1.1) or glucoamylase (E.C. 3.2.1.3) is well understood (Supplementary Material). The kinetic characterization of oligosaccharide digestion now enables prediction of the time course of glucose production in the digestion of any combination of oligosaccharides, likely providing a better understanding of the time courses of processes that occur in the distal regions of the human digestive tract; this will be possible once amounts (V_{max} values) of each glycohydrolase and their K_m values are determined.

A two-stage model with Michaelis–Menten kinetics, which described hydrolysis of the soluble portion of rice starch granules, and the insoluble portion with an exponential model, was successfully applied to many starch digestion mixtures in the present work. Simulations using the two-stage model accurately described the entire time course of regular-maize starch digestion. Development of a two-stage model with a mechanistic basis for the rate equations led to a better understanding of the functional consequences of the interaction of hydrolytic enzymes with partially solubilized starch. Research by our group has currently been advanced to include partially gelatinized samples. Recent results support the hypothesis that the solvated portion of the starch granule breaks down according to Michaelis–Menten kinetics, and the insoluble core follows an exponential rate law.

As our kinetic models quantitatively explain the digestion of starch, application of the two/multistage model should help to elucidate features and nutritional variations of granular starch from any food source. The models should also lead to a better understanding of nutritionally important differences between starch varieties, as well as a better understanding of the effects of hydrothermal treatment, and starch modifications on digestibility. These insights will be valuable for the quantitative analysis of diets and the prediction of the kinetics of glucose supply in the management of the various diseases noted in the Introduction.

Acknowledgments

PWK and RGG gratefully acknowledge the support of Australian Research Council grants DP0877789 and DP0985694, respectively.

Appendix A. Supplementary data

Supplementary data associated with this article can be found, in the online version, at doi:10.1016/j.carbpol.2010.10.042.

References

Akerberg, C., Zacchi, G., Torto, N., & Gorton, L. (2000). A kinetic model for enzymatic wheat starch saccharification. *Journal of Chemical Technology and Biotechnology*, *75*, 306–314.

Al-Rabadi, G. J. S., Gilbert, R. G., & Gidley, M. J. (2009). Effect of particle size on kinetics of starch digestion in milled barley and sorghum grains by porcine α-amylase. *Journal of Cereal Science*, *50*, 198–204.

Amato, M. E., Ansanelli, G., Fisichella, S., Lamanna, R., Scarlata, G., Sobolev, A. P., et al. (2004). Wheat flour enzymatic amylolysis monitored by in situ ^{1}H NMR spectroscopy. *Journal of Agricultural and Food Chemistry*, *52*, 823–831.

Ao, Z., Simsek, S., Zhang, G., Venkatachalam, M., Reuhs, B. L., & Hamaker, B. R. (2007). Starch with a slow digestion property produced by altering its chain length, branch density, and crystalline structure. *Journal of Agricultural and Food Chemistry*, *55*, 4540–4547.

Apar, D. K, & Ozbek, B. (2007). Estimation of kinetic parameters for rice starch hydrolysis inhibited by added materials. *Chemical Engineering Communications*, *194*, 334–344.

Batey, I. L., & Curtin, B. M. (1996). Measurement of amylose/amylopectin ratio by high-performance liquid chromatography. *Starch/Staerke*, *48*, 338–344.

Beltrame, P. L., Carniti, P., Focher, B., Marzetti, A., Santoro, C., Heyraud, A., et al. (1987). Kinetics of enzymic hydrolysis of malto-oligosaccharides. A comparison with acid hydrolysis. *Carbohydrate Research*, *166*, 71–83.

BeMiller, J. N., & Whistler, R. L. (2009). *Starch chemistry and technology*. London: Academic Press, Elsevier.

Birch, G. G., & Karim, R. (1992). Apparent molar volumes and proton-NMR relaxation values of glucose syrups. *Journal of the Science of Food and Agriculture*, *58*, 563–568.

Birkett, A. M., & Brown, I. L. (2008). Resistant starch and health. *Technology of Functional Cereal Products*, 63–85.

Brand-Miller, J. C., Holt, S. H. A., Pawlak, D. B., & McMillan, J. (2002). Glycemic index and obesity. *American Journal of Clinical Nutrition*, *76*, 281S–285S.

Chapman, B. E., Beilharz, G. R., York, M. J., & Kuchel, P. W. (1982). Endogenous phospholipase and choline release in human erythrocytes: a study using ^{1}H-NMR spectroscopy. *Biochemical and Biophysical Research Communications*, *105*, 1280–1287.

Chou, W.-I., Pai, T.-W., Liu, S.-H., Hsiung, B.-K., & Chang, M. D. (2006). The family 21 carbohydrate-binding module of glucoamylase from *Rhizopus oryzae* consists of two sites playing distinct roles in ligand binding. *Biochemical Journal*, *396*, 469–477.

Chung, H.-J., Lim, H. S., & Lim, S.-T. (2006). Effect of partial gelatinization and retrogradation on the enzymatic digestion of waxy rice starch. *Journal of Cereal Science*, *43*, 353–359.

Chung, H.-J., Yoo, B., & Lim, S.-T. (2005). Effects of physical aging on thermal and mechanical properties of glassy normal corn starch. *Starch/Staerke*, *57*, 354–362.

Conway, R. L., & Hood, L. F. (1976). Comparison of spectrodensitometric and colorimetric methods for quantifying starch hydrolysis products separated by thin-layer chromatography. *Journal of Chromatography*, *129*, 415–419.

Cornish-Bowden, A., & Hofmeyer, J.-H. S. (2005). Enzymes in context: kinetic characterization of enzymes for systems biology. *Biochemist*, *27*, 11–14.

Dona, A. C., Pages, G., Gilbert, R. G., Gaborieau, M., & Kuchel, P. W. (2009). Kinetics of in vitro digestion of starches monitored by time-resolved ^{1}H nuclear magnetic resonance. *Biomacromolecules*, *10*, 638–644.

Dona, A. C., Pages, G., Gilbert, R. G., & Kuchel, P. W. (2010). Digestion of starch: In vivo and in vitro kinetic models used to characterise oligosaccharide or glucose release. *Carbohydrate Polymers*, *80*, 599–617.

Dona, A., Yuen, C.-W. W., Peate, J., Gilbert, R. G., Castignolles, P., & Gaborieau, M. (2007). A new NMR method for directly monitoring and quantifying the dissolution kinetics of starch in DMSO. *Carbohydrate Research*, *342*, 2604–2610.

Eerlingen, R. C., Jacobs, H., & Delcour, J. A. (1994). Enzyme-resistant starch. V. Effect of retrogradation of waxy maize starch on enzyme susceptibility. *Cereal Chemistry*, *71*, 351–355.

Eisenthal, R., & Cornish-Bowden, A. (1974). Direct linear plot. New graphical procedure for estimating enzyme kinetic parameters. *Biochemical Journal*, *139*, 715–720.

Englyst, H. N., Kingman, S. M., & Cummings, J. H. (1992). Classification and measurement of nutritionally important starch fractions. *European Journal of Clinical Nutrition*, *46*, 33–50.

Farhat, I. A., Protzmann, J., Becker, A., Valles-Pamies, B., Neale, R., & Hill, S. E. (2001). Effect of the extent of conversion and retrogradation on the digestibility of potato starch. *Starch/Staerke*, *53*, 431–436.

Fassler, C., Arrigoni, E., Venema, K., Hafner, V., Brouns, F., & Amado, R. (2006). Digestibility of resistant starch containing preparations using two in vitro models. *European Journal of Nutrition*, *45*, 445–453.

Fraser-Reid, B. O., Tatsuta, K., & Thiem, J. (Eds.). (2001). *Glycoscience: Chemistry and chemical biology, Vol. 2*. Berlin: Springer.

Frei, M., Siddhuraju, P., & Becker, K. (2003). Studies on the in vitro starch digestibility and the glycemic index of six different indigenous rice cultivars from the Philippines. *Food Chemistry*, *83*, 395–402.

French, D., & Knapp, D. W. (1950). The maltase of *Clostridium acetobutylicum*. Its specificity range and mode of action. *Journal of Biological Chemistry*, *187*, 463–471.

Fried, M., Abramson, S., & Meyer, J. H. (1987). Passage of salivary amylase through the stomach in humans. *Digestive Diseases and Sciences*, *32*, 1097–1103.

Fujii, M., & Kawamura, Y. (1985). Synergistic action of α-amylase and glucoamylase on hydrolysis of starch. *Biotechnology and Bioengineering*, *27*, 260–265.
Goni, I., Garcia-Alonso, A., & Saura-Calixto, F. (1997). A starch hydrolysis procedure to estimate glycemic index. *Nutrition Research (New York)*, *17*, 427–437.
Granfeldt, Y., Eliasson, A. C., & Bjorck, I. (2000). An examination of the possibility of lowering the glycemic index of oat and barley flakes by minimal processing. *The Journal of Nutrition*, *130*, 2207–2214.
Gubern, G., Canalias, F., & Gella, F. J. (1995). Determination of α-amylase activity: methods comparison and commutability study of several control materials. *Clinical Chemistry (Washington, DC)*, *41*, 435–438.
Guraya, H. S., James, C., & Champagne, E. T. (2001). Effect of cooling, and freezing on the digestibility of debranched rice starch and physical properties of the resulting material. *Starch/Staerke*, *53*, 64–74.
Haralampu, S. G. (2001). In-vivo and in-vitro digestion of resistant starch. *Advanced Dietary Fibre Technology*, 413–423.
Heitmann, T., Wenzig, E., & Mersmann, A. (1997). Characterization of three different potato starches and kinetics of their enzymic hydrolysis by an α-amylase. *Enzyme and Microbial Technology*, *20*, 259–267.
Heymann, H., Breitmeier, D., & Guenther, S. (1995). Human small intestinal sucrase-isomaltase: different binding patterns for malto- and isomaltooligosaccharides. *Biological Chemistry Hoppe-Seyler*, *376*, 249–253.
Hill, G. A., Macdonald, D. G., & Lang, X. (1997). α-Amylase inhibition and inactivation in barley malt during cold starch hydrolysis. *Biotechnology Letters*, *19*, 1139–1141.
Himmelreich, U., Drew, K. N., Serianni, A. S., & Kuchel, P. W. (1998). ^{13}C NMR studies of vitamin C transport and its redox cycling in human erythrocytes. *Biochemistry*, *37*, 7578–7588.
Holm, J., Lundquist, I., Bjorck, I., Eliasson, A. C., & Asp, N. G. (1988). Degree of starch gelatinization, digestion rate of starch in vitro, and metabolic response in rats. *American Journal of Clinical Nutrition*, *47*, 1010–1016.
Jenkins, D. J. A., Kendall, C. W. C., Augustin, L. S. A., Franceschi, S., Hamidi, M., Marchie, A., et al. (2002). Glycemic index: overview of implications in health and disease. *American Journal of Clinical Nutrition*, *76*, 266S–273S.
Kazaz, M. A., Desseaux, V., Marchis-Mouren, G., Prodanov, E., & Santimone, M. (1998). The mechanism of porcine pancreatic α-amylase. Inhibition of maltopentaose hydrolysis by acarbose, maltose and maltotriose. *European Journal of Biochemistry*, *252*, 100–107.
Kennett, E. C., Ogawa, E., Agar, N. S., Godwin, I. R., Bubb, W. A., & Kuchel, P. W. (2005). Investigation of methemoglobin reduction by extracellular NADH in mammalian erythrocytes. *International Journal of Biochemistry & Cell Biology*, *37*, 1438–1445.
Kerr, R. W., Cleveland, F. C., & Katzbeck, W. J. (1951). The action of amyloglucosidase on amylose and amylopectin. *Journal of Amercan Chemical Society*, *73*, 3916–3921.
Kimura, A., & Robyt, J. F. (1995). Reaction of enzymes with starch granules: kinetics and products of the reaction with glucoamylase. *Carbohydrate Research*, *277*, 87–107.
Kimura, A., & Robyt, J. F. (1996a). Reaction of enzymes with starch granules: enhanced reaction of glucoamylase with gelatinized starch granules. *Carbohydrate Research*, *288*, 233–240.
Kimura, A., & Robyt, J. F. (1996b). Reaction of enzymes with starch granules: reaction of isoamylase with native and gelatinized granules. *Carbohydrate Research*, *287*, 255–261.
King, G. F., & Kuchel, P. W. (1984). A proton NMR study of iminodipeptide transport and hydrolysis in the human erythrocyte. Possible physiological roles for the coupled system. *Biochemical Journal*, *220*, 553–560.
King, G. F., Middlehurst, C. R., & Kuchel, P. W. (1986). Direct NMR evidence that prolidase is specific for the trans isomer of imidodipeptide substrates. *Biochemistry*, *25*, 1054–1062.
Komaki, T., Matsuba, Y., Okamoto, N., & Sato, T. (1959). Enzymic hydrolysis of starch. IV. Production of glucose by using amylolytic enzyme prepared from fungi. *Denpun Kogyo Gakkaishi*, *6*, 98–105.
Komolprasert, V., & Ofoli, R. Y. (1991). Starch hydrolysis kinetics of *Bacillus licheniformis* α-amylase. *Journal of Chemical Technology and Biotechnology*, *51*, 209–223.
Kruger, J. E., & Marchylo, B. A. (1985). A comparison of the catalysis of starch components by isoenzymes from the two major groups of germinated wheat α-amylase. *Cereal Chemistry*, *62*, 11–18.
Kuchel, P. W., & Ralston, G. B. (1992). *Schaum's outline of theory and problems of biochemistry: Enzymes and reaction kinetics* (2nd edn.). NY: McGraw-Hill. Chapter 9
Larner, J., & McNickle, C. M. (1955). Gastrointestinal digestion of starch. I. The action of oligo-1,6-glucosidase on branched saccharides. *Journal of Biological Chemistry*, *215*, 723–736.
Leloup, V. M., Colonna, P., & Ring, S. G. (1991). α-Amylase adsorption on starch crystallites. *Biotechnology and Bioengineering*, *38*, 127–134.
Lim, S.-T., Lee, J.-H., Shin, D.-H., & Lim, H. S. (1999). Comparison of protein extraction solutions for rice starch isolation and effects of residual protein content on starch pasting properties. *Starch/Staerke*, *51*, 120–125.
Manelius, R., Qin, Z., Avall, A. K., Andtfolk, H., & Bertoft, E. (1997). The mode of action of granular wheat starch by bacterial α-amylase. *Starch/Staerke*, *49*, 142–147.
McCleary, B. V. (2007). An integrated procedure for the measurement of total dietary fibre (including resistant starch), non-digestible oligosaccharides and available carbohydrates. *Analytical and Bioanalytical Chemistry*, *389*, 291–308.
McLaren, A. D. (1963). Enzyme reactions in structurally restricted systems. IV. The digestion of insoluble substrates by hydrolytic enzymes. *Enzymologia*, *26*, 237–246.
Meiboom, S., & Gill, D. (1958). Modified spin-echo method for measuring nuclear relaxation times. *Review of Scientific Instruments*, *29*, 688–691.
Miah, M. N. N., & Ueda, S. (1977). Multiplicity of glucoamylase of *Aspergillus oryzae*. Part 2. Enzymic and physicochemical properties of three forms of glucoamylase. *Staerke*, *29*, 235–239.
Michaelis, L., & Menten, M. L. (1913). Kinetics of invertase action. *Biochemische Zeitschrift*, *49*, 333–369.
Middlehurst, C. R., King, G. F., Beilharz, G. R., Hunt, G. E., Johnson, G. F. S., & Kuchel, P. W. (1984). Studies of rat brain metabolism using proton nuclear magnetic resonance: spectral assignments and monitoring of prolidase, acetylcholinesterase, and glutaminase. *Journal of Neurochemistry*, *43*, 1561–1567.
Moreira, F. G, Lenartovicz, V., & Peralta, R. M. (2004). A thermostable maltose-tolerant α-amylase from *Aspergillus tamarii*. *Journal of Basic Microbiology*, *44*, 29–35.
Mukerjea, R., Slocum, G., Mukerjea, R., & Robyt, J. F. (2006). Significant differences in the activities of α-amylases in the absence and presence of polyethylene glycol assayed on eight starches solubilized by two methods. *Carbohydrate Research*, *341*, 2049–2054.
Mulquiney, P. J., & Kuchel, P. W. (2003). *Modelling metabolism with mathematica*. Boca Raton, FL: CRC Press.
Nitta, Y., Kunikata, T., & Watanabe, T. (1979). Kinetic study of soybean β-amylase. The effect of pH. *Journal of Biochemistry*, *85*, 41–45.
Noda, T., Isono, N., Krivandin, A. V., Shatalova, O. V., Blaszczak, W., & Yuryev, V. P. (2009). Origin of defects in assembled supramolecular structures of sweet potato starches with different amylopectin chain-length distribution. *Carbohydrate Polymers*, *76*, 400–409.
Ohnishi, M. (1971). Studies of the interaction of substrate analogs with bacterial liquefying α-amylase by means of spectrophotometry and steady state kinetics. *Journal of Biochemistry*, *69*, 181–189.
Park, J. T., & Rollings, J. E. (1995). Effects of substrate branching characteristics on kinetics of enzymatic depolymerization of mixed linear and branched polysaccharides: II. Amylose/glycogen α-amylolysis. *Biotechnology and Bioengineering*, *46*, 36–42.
Pastrana, L., Gonzalez, M., Miron, J., & Murado, M. A. (1998). A new device for measuring diffusional restrictions and modeling substrate inhibition in a starch-glucoamylase system. *Biotechnology Letters*, *20*, 127–130.
Raftos, J. E., Whillier, S., Chapman, B. E., & Kuchel, P. W. (2007). Kinetics of uptake and deacetylation of N-acetylcysteine by human erythrocytes. *International Journal of Biochemistry & Cell Biology*, *39*, 1698–1706.
Roberts, S. B. (2000). High-glycemic index foods, hunger, and obesity: is there a connection? *Nutrition Reviews*, *58*, 163–169.
Robyt, J. F. (1998). *Essentials of carbohydrate chemistry*. NY: Springer.
Shiotsubo, T. (1983). Study of starch gelatinization. Part I. Starch gelatinization at different temperatures as measured by an enzymic digestion method. *Agricultural and Biological Chemistry*, *47*, 2421–2425.
Sim, L., Quezada-Calvillo, R., Sterchi, E. E., Nichols, B. L., & Rose, D. R. (2008). Human intestinal maltase-glucoamylase: crystal structure of the N-terminal catalytic subunit and basis of inhibition and substrate specificity. *Journal of Molecular Biology*, *375*, 782–792.
Singh, N., Isono, N., Srichuwong, S., Noda, T., & Nishinari, K. (2008). Structural, thermal and viscoelastic properties of potato starches. *Food Hydrocolloids*, *22*, 979–988.
Soini, H. A., & Novotny, M. V. (1999). Capillary electrophoresis in starch analysis. *ACS Symposium Series*, *737*, 317–328.
Sopade, P. A., & Gidley, M. J. (2009). A rapid in-vitro digestibility assay based on glucometry for investigating kinetics of starch digestion. *Starch/Staerke*, *61*, 245–255.
Svihus, B., Uhlen, A. K., & Harstad, O. M. (2005). Effect of starch granule structure, associated components and processing on nutritive value of cereal starch: a review. *Animal Feed Science and Technology*, *122*, 303–320.
Thompson, D. B. (2000). On the non-random nature of amylopectin branching. *Carbohydrate Polymers*, *43*, 223–239.
Thornley, S., McRobbie, H., Eyles, H., Walker, N., & Simmons, G. (2008). The obesity epidemic: is glycemic index the key to unlocking a hidden addiction? *Medical Hypotheses*, *71*, 709–714.
Topping, D. L., Bajka, B. H., Bird, A. R., Clarke, J. M., Cobiac, L., Conlon, M. A., et al. (2008). Resistant starches as a vehicle for delivering health benefits to the human large bowel. *Microbial Ecology in Health and Disease*, *20*, 103–108.
Tueting, W., Albrecht, G., Volkert, B., & Mischnick, P. (2004). Structure analysis of carboxymethyl starch by capillary electrophoresis and enzymic degradation. *Starch/Staerke*, *56*, 315–321.
Wang, J.-P., Zeng, A.-W., Liu, Z., & Yuan, X.-G. (2006). Kinetics of glucoamylase hydrolysis of corn starch. *Journal of Chemical Technology and Biotechnology*, *81*, 727–729.
Werner, R., & Keilich, G. (1965). An enzymatic method on kinetic studies of endohydrolases: activity determination of α-amylase. *Biochemische Zeitschrift*, *342*, 226–235.
Whillier, S., Raftos, J. E., Chapman, B. E., & Kuchel, P. W. (2009). Role of N-acetylcysteine and cystine in glutathione synthesis in human erythrocytes. *Redox Report*, *14*, 115–124.
Whistler, R. L., BeMiller, J. N., & Paschall, E. F. (1984). *Starch Chemistry and Technology*. NY: Academic Press.
Wolever, T. M. S., Mehling, C., Chiasson, J. L., Josse, R. G., Leiter, L. A., Maheux, P., et al. (2008). Low glycaemic index diet and disposition index in type 2 diabetes (the Canadian trial of carbohydrates in diabetes): a randomised controlled trial. *Diabetologia*, *51*, 1607–1615.

Yoon, S.-H., & Robyt, J. F. (2003). Study of the inhibition of four alpha amylases by acarbose and its 4IV-α -maltohexaosyl and 4IV-α -maltododecaosyl analogues. *Carbohydrate Research*, *338*, 1969–1980.

Yoshikuni, Y. (1988). Inhibition of intestinal α-glucosidase activity and postprandial hyperglycemia by moranoline and its N-alkyl derivatives. *Agricultural and Biological Chemistry*, *52*, 121–128.